Cleland, W. W. (1975) *Biochemistry 14*, 3220-3224.
Cohn, M., & Hu, A. (1978) *Proc. Natl. Acad. Sci. U.S.A. 75*, 200-203.
DeBrosse, C. W., & Villafranca, J. J. (1983) *Magnetic Resonance in Biology* (Cohen, J. S., Ed.) pp 1-51, Wiley, New York.
Ginsburg, A., Yeh, J., Hennig, S. B., & Denton, M. D. (1970) *Biochemistry 9*, 633-648.
Krishnaswamy, P. R., Pamiljans, V., & Meister, A. (1962) *J. Biol. Chem. 237*, 2932-2940.
Lowry, O. H., Rosebraugh, N. J., Farr, A. L., & Randall, R. J. (1951) *J. Biol. Chem. 193*, 265-275.
Meek, T. D., & Villafranca, J. J. (1980) *Biochemistry 19*, 5513-5519.
Meek, T. D., Johnson, K. A., & Villafranca, J. J. (1982) *Biochemistry 21*, 2158-2167.
Meister, A. (1968) *Adv. Enzymol. Relat. Areas Mol. Biol. 31*, 183-218.
Midelfort, C. F., & Rose, I. A. (1976) *J. Biol. Chem. 251*, 5881-5887.
Miller, R. E., Shelton, E., & Stadtman, E. R. (1974) *Arch. Biochem. Biophys. 163*, 155-171.
Raushel, F. M., & Garrard, L. J. (1984) *Biochemistry 23*, 1791-1795.
Risley, J. M., & Van Etten, R. L. (1978) *J. Labelled Compd. Radiopharm. 15*, 533-538.
Timmons, R. B., Rhee, S. G., Luterman, D. L., & Chock, P. B. (1974) *Biochemistry 13*, 4479-4484.
Tsuda, Y., Stephani, R. A., & Meister, A. (1971) *Biochemistry 10*, 3186-3189.
Wedler, F. C., & Boyer, P. D. (1972) *J. Biol. Chem. 247*, 984-992.
Woolfolk, C. A., Shapiro, B. M., & Stadtman, E. R. (1966) *Arch. Biochem. Biophys. 116*, 177-192.

Circular Dichroism Studies on Single Chinese Hamster Cells†

Marcos F. Maestre*
Biology and Medicine Division, Lawrence Berkeley Laboratory, Berkeley, California 94720
Gary C. Salzman and Robert A. Tobey
Los Alamos National Laboratory, Los Alamos, New Mexico 87545
Carlos Bustamante
Chemistry Department, The University of New Mexico, Albuquerque, New Mexico 87177
Received December 18, 1984

ABSTRACT: The circular dichroism (CD) and circular intensity differential scattering (CIDS) contributions to the CD of single Chinese hamster (CHO) cells have been measured as a function of the position in the cell cycle. The data are analyzed in three main spectral regions: (1) the region above 290 nm (scattering region), (2) the 250-290-nm regions (nucleic acid absorption region), and (3) the region below 240 nm (protein absorption region). The results show that CD/CIDS microspectrophotometry is a good indicator of the cell cycle phase. The results are consistent with the view that chromatin is organized in chiral superstructures which differentially scatter circularly polarized light. These structures appear highly specific and repeatable as the cell passes through its cycle.

Circular dichroism (CD) is a spectroscopic technique sensitive to primary, secondary, and tertiary structures of biological macromolecules. It measures the difference in absorption cross section exhibited by a sample when it is illuminated successively with right- and left-circularly polarized light. The technique has been applied to the study of structures ranging from small chiral molecules, of the order of nucleic acid monomers, to structures as large as intact bacterial cells, cell nuclei, and eukaryotic cells in solutions (Tinoco et al., 1980). Interpretation of results had been reasonably straightforward in cases of simple chiral organizations, such as small optically active molecules. However, results have been complicated by the presence of scattering contributions and distribution effects (Duysens, 1957) in cases of large organizations such as red blood cell membranes, bacteriophages, and intact eukaryotic cells and cell nuclei. These scattering contributions are manifestations of preferential light scattering of right- or left-circularly polarized light, which reflects the higher order chiral structure of the material measured.

The signal measured in a circular dichrograph along the transmitted beam is (Bustamante et al., 1983)

$$\frac{I_R - I_L}{I_R + I_L} = \frac{2.303(\epsilon_L - \epsilon_R)cl}{2} + \frac{\sigma_R(0) - \sigma_L(0)}{2r^2 + \sigma_L(0) + \sigma_R(0)} \quad (1)$$

where I_R and I_L are the intensities transmitted for right- (R) and left-circularly (L) polarized light and $\sigma_R(0)$ and $\sigma_L(0)$ are the scattering cross sections of the sample in the forward direction. r is the distance of the detector from the sample. The first term involves the difference in extinction coefficients, i.e., the circular dichrosim. ϵ_R and ϵ_L are the extinction coefficients for right- and left-circularly polarized light, c is

†This work was supported in part by National Institutes of Health Grants A1082447 (M.F.M.), GM26857 (G.C.S.), and GM32543 (C.B.), by a Searle Scholarship awarded to C.B., and by a grant from the Health and Environment Research, Office of Energy Research, U.S. Department of Energy, under Contract DE-AC03-765F00098.

0006-2960/85/0424-5152$01.50/0

the concentration, and l is the path length through the sample. It can be shown that these extinction coefficients have two contributions, absorption (a) and scattering (s):

$$\epsilon_L - \epsilon_R = (a_L - a_R) + (s_L - s_R) \quad (2)$$

The first term in eq 2 is the usual one considered when a chiral system is measured whose size is much smaller than the wavelength of light and scatters light weakly. The circular differential scattering coefficient ($s_L - s_R$) is related to the integral over all angles of the angle-dependent scattering cross section:

$$s_L - s_R = \frac{2\pi N_0}{2303} \int_0^{2\pi} d\phi \int_0^{\pi} [\sigma_{sca,L}(\theta) - \sigma_{sca,R}(\theta)] \sin\theta \, d\theta \quad (3)$$

This term is a measure of the differential scattering of the particle. It is a function of the wavelength, and chiral parameters, and of the arrangement of the polarizability tensor of the scattering subunits. It also depends on the orientation of the object with respect to the light beam and on the orientation and acceptance angle of the detection optics. The differential scattering contributions appears as CD spectral "tails", i.e., apparent CD outside the absorption bands. Recently, there has been an increased understanding of the theoretical basis of these anomalies of CD curves [see Tinoco et al. (1982) and Bustamante et al. (1983, 1984, 1985) for a review of the present state of understanding the phenomenon]. Instead of considering the anomalous signals as artifacts of the measuring process, this theoretical scheme has permitted the first angle-resolved measurements of the circular intensity differential scattering (CIDS) (Maestre et al., 1982).

The efficiency of a particle to scatter preferentially right- or left-circularly polarized light is measured by the CIDS ratio (Bustamante et al., 1980a):

$$\mathrm{CIDS}(\theta,\phi) = \frac{I_L(\theta,\phi) - I_R(\theta,\phi)}{I_L(\theta,\phi) + I_R(\theta,\phi)} \quad (4)$$

where $I_L(\theta,\phi)$ and $I_R(\theta,\phi)$ are the scattered intensities at position θ,ϕ in space due to incident right- (R) or left-circularly (L) polarized light.

Previously, the CD studies have been on solutions or suspensions of these materials; i.e., the signals measured are the average signals of the population. In most cases, the population average represents well the properties of each of the members of the the group due to population homogeneity. This is not true for populations such as a collection of exponentially growing mammalian cells, since the cells comprising the population are distributed throughout the life cycle. Instrumentation capable of characterizing the optical properties of microscopic objects, i.e., individual cells in a given population, is of great interest for two reasons: (1) it is an analytical technique that allows the identification of the stage of the cell along its life cycle; and (2) it also provides information regarding the structural changes that the cell undergoes during the cycle. To study the optical activity properties of individual cells, a circular dichroism microspectrophotometer was developed by Maestre & Katz, (1982). The instrument can measure simultaneously the CD and absorbance spectra in the wavelength region of 200–800 nm. Preliminary measurements of DNA microcrystals (Downing & Maestre, 1979) and of human lymphocytes and red blood cells have shown that the measurements are feasible and that a good signal to noise ratio is obtained (Maestre & Katz, 1982).

In this work, we present the first measurements of the CD and CIDS spectral contributions on single Chinese hamster tissue culture cells (CHO line) as a function of position in the cell cycle. We show that there are distinct spectra associated with the different phases of the cell cycle.

Materials and Methods

Line CHO Chinese hamster cells were grown in F10 medium supplemented with 15% neonate calf serum and antibiotics. Cells in mitois were prepared by mitotic selection in the manner described previously (Tobey et al., 1967). An aliquot of detached mitotic cells was centrifuged, and the cell pellet was resuspended in 50% ethanol in phosphate-buffered saline (PBS); this sample contained >95% mitotic cells and represents the "M-phase population". A second aliquot of detached mitotic cells was pelleted, and the cells were suspended in fresh, warm F10 medium. Following incubation at 37 °C for 2 h, the cells were spun down and resuspended in 50% ethanol in PBS; this sample, the "G_1-rich population", contained >99% of the cells in the G_1-phase division cycle, determined by flow cytometric analysis (Cram & Holm, 1973; Crissman & Tobey, 1974).

Mid- to late-interphase cells were obtained by first synchronizing the cells in very early S phase by a procedure combining isoleucine deprivation with hydroxyurea treatment (Tobey & Crissman, 1972). Following resuspension of the cells in drug-free medium, one aliquot was harvested after incubation for 1 h at 37 °C when nearly 90% of the cells were replicating DNA (with the remainder still in G_1); this sample constitutes the "S-rich population". A second aliquot of cell synchronized by the isoleucine–hydroxyurea protocol was incubated in drug-free medium for 5.5 h prior to resuspension in 50% ethanol in PBS; slightly more than half the cells comprising the "G_2-rich population" were in the G_2 phase of the cell cycle, with the remaining cells distributed in G_1 and S. Although two different methods of synchronization were utilized in this report, there is no evidence that the method of synchronization greatly affects the parameters measured in this series of experiments (unpublished observations). No removal of the RNA in the cell was attempted. No measurements were done on isolated nuclei from the cells.

Measurements

A total of 398 cells were measured in the CD/CIDS microscope. Cells were scanned over the wavelength with a 32-power and/or 100-power objective. In 39 cases, the same cell was measured with both the 32- and 100-power objective to do a comparative study of the scattering component of each individual cell. The cells in this group were used to perform a statistical analysis (see below) to group together similar spectra. The results of this analysis (presented here) confirm the conclusions arrived at by inspection of the data from the rest of the cells.

The measurement procedure consisted of positioning a randomly selected cell in the field of view so that its nucleus was centered in a 10-μm diameter aperture. In most cases, some of the cytoplasm was included in the signal, and in particular for some cells in the mitotic phase with no defined nuclear region, the whole cell was used. The CD/CIDS spectrum was scanned from 330 to 220 nm, and the data were digitized with 1-nm intervals. The positioning of the cell was checked at the end of each scan. Background scans were run for every cell by placing the 10-μm diameter aperture over a clear area adjacent to the scanned cell. Data were considered reliable only for photomultiplier tube dynode voltages below 800 V.

CD/CIDS was measured by the microscope as a function of cell cycle position. As stated above, each of 39 group cells was scanned with a 32-power and 100-power objective. This

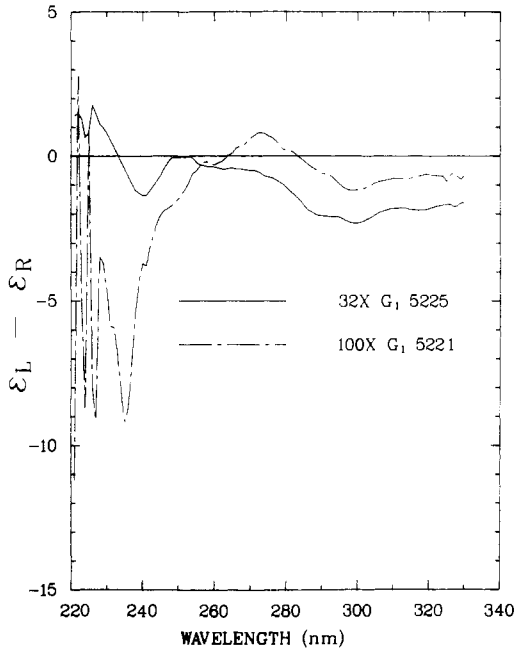

FIGURE 1: CD/CIDS values as a function of wavelength for a single cell from the G_1 aliquot for both 100× and 32× magnifications.

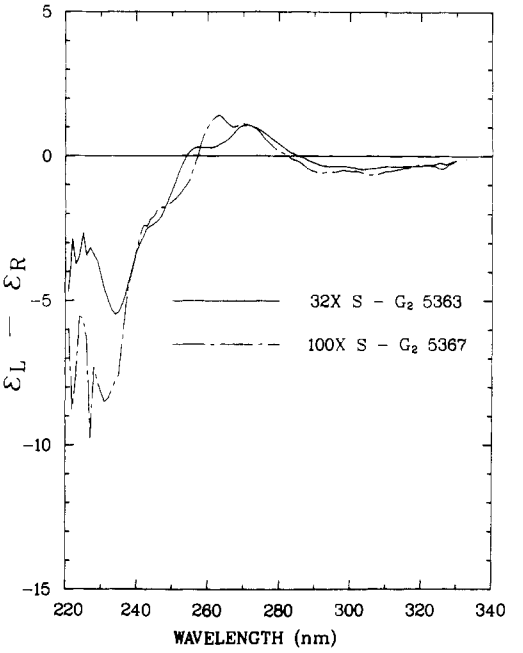

FIGURE 2: CD/CIDS values as a function of wavelength for a single cell from the S–G_2 cluster for both 100× and 32× magnifications.

procedure is important because the two objectives capture different amounts of scattered light. The acceptance half-angle at the 32× objective (N.A. 0.4 glycerol immersion) is 15.5°, and that of the 100× objective (N.A. 1.25 glycerol immersion) is 56.4°. The differences in the CD/CIDS data taken with the two objectives provide a measure of the integrated CIDS scattering angular range from ±15.5° to ±56.4° from the forward direction.

Signal Processing. Each CD/CIDS scan was averaged by summing up to 2032 times for each 10-Å interval in the spectra. The stored data were then smoothed by third-degree 13-point interpolation routine (Tomlinson, 1968). The data are plotted as CD spectra per cell unit since it is relative to the particular position in the cell cycle.

To check for possible alteration of the signal due to damage to the cell structure from UV irradiation, repeated scans were done on selected cells. There was little or no change in the CD/CIDS signal for up to three consecutive scans on the same cell.

RESULTS

Measurements at both magnifications were made on a total of single CHO cells randomly selected from the four aliquots: 18 from G_1, 5 from S, 2 from G_2, and 14 from M. Figure 1 shows an example of the two measurements on the single cell from the G_1-rich population. The dramatic differences between these two different magnifications of CD/CIDS scans of the same cell imply that there is a significant differential scattering of the circularly polarized light of the scattering angular range between ±15.5° and ±56.4°. At around 235 nm, the 32× curve passes through zero while the 100× curve is near its negative extreme. This implies that a 235 nm the CIDS is positive in the angular region from ±15.5° to ±56.4°. Similarly, the CIDS is negative in the wavelength region near 320 nm. Figure 2 shows an example from the S-phase aliquot. The curves are nearly identical except in the region below 240 nm. Above 240 nm, there is little CIDS in the angular range between ±15.5° and ±56.4°.

It is important to state that we are reasonably confident that the measurements of the M and G_1-rich cells reflect the properties of those phases of the cell cycle but that 1 in 10 in the S-rich and nearly 1 in 2 in the G_2-rich population are the wrong cells. The random sampling from the synchronized aliquots selected cells from several phases of the cell cycle even within one aliquot. Therefore, a mathematical technique known as cluster analysis (Goad, 1978; Salzman et al., 1975) was used to group together similar scans. Three regions were selected in each of the 39 scans: the protein region (221–240 nm); the DNA region (250–290 nm)f and the scatter region (291–330 nm). For each cell, the CD/CIDS data were averaged in each of the three regions, and a data set was created consisting of an array of 39 three-element vectors. Each vector contained the averaged data for one cell. The clustering algorithm uses a *K*-nearest-neighbor method to group together nearby points in this three-dimensional space. The analysis found three clusters with membership varying from 24 to 7 cells. The scans in each cluster were averaged together. The

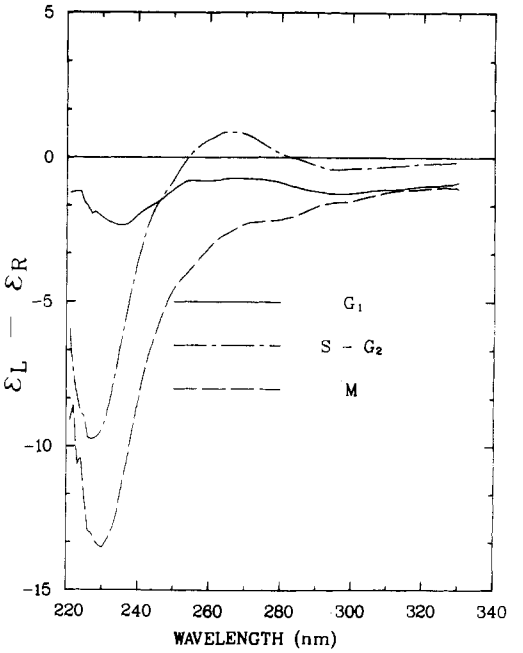

FIGURE 3: Average CD/CIDS values for the three clusters obtained from the 32× magnification of raw data as a function of wavelength.

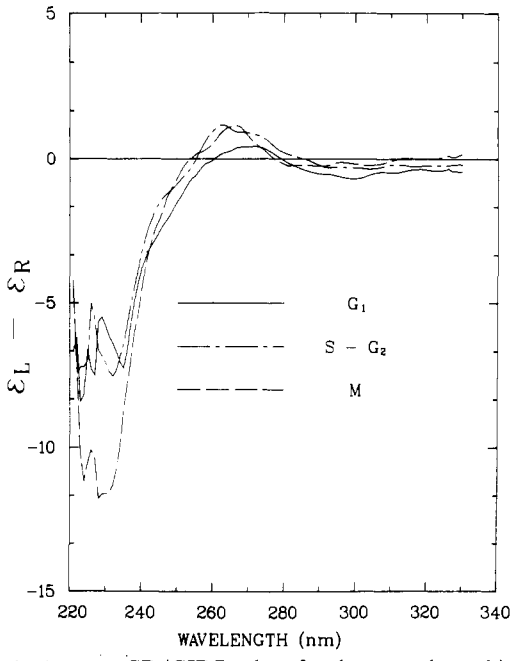

FIGURE 4: Average CD/CIDS values for the same three clusters as in Figure 3 but using the 100× data.

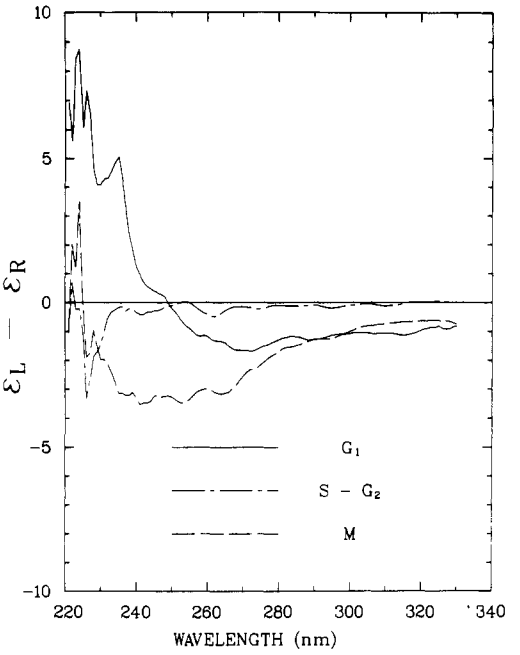

FIGURE 5: Average values of the difference CD/CIDS spectra obtained by subtracting the 100× data for each cell in a cluster from the 32× data for the cell and averaging the resulting data for each cluster. This is essentially the differential scattering contribution to CD/CIDS as a function of wavelength.

results are shown in Figure 3 for 32× data. In the 24-member cluster, we have labeled G_1; the clustering algorithm grouped together 18 scans from the G_1 aliquot and 6 scans from the M aliquot. This is expected since the M-phase population is obtained by releasing the M-phase population from the cold block. In the eight-member cluster, we have labeled S–G_2, and the clustering grouped together five cells from the S-phase aliquot, two from the G_2 aliquot, and one from the M-phase aliquot. The seven-member cluster labeled M contains only cells from the M-phase aliquot. Figure 3 shows dramatic changes in the CD/CIDS spectra across the cell cycle particularly at the shorter wavelengths.

Figure 4 shows the data for the same three clusters of cells but using the scans with the 100× objective. Here the CD/CIDS values are nearly the same for all three clusters except at the shortest wavelengths, implying that the 100× objective collects most of the differentially scattered light, eliminating in this way the "tails" outside the absorption band.

Figure 5 shows the difference CD/CIDS spectra computed by subtracting the data in Figure 4 from those in Figure 3 to obtain curves showing the CIDS in the forward-scattering cone in the angular range between ±15.5° and ±56.4° for each of the three clusters. These differential scattering curves are the significant data that will be interpreted and from which conclusions will be drawn in this work.

Discussion

While the microscopic CD/CIDS measurements may provide a unique approach to cell cycle analysis, the structures of the biologically interesting organelles responsible for producing the measured effects are not know at present. Consequently, no models can be used to compute the integrated differential scattering contributions present in these measurements. However, general conclusions from a qualitative point of view can be obtained, with some insight on the structures that may produce the changes.

The spectra can be analyzed roughly in three wavelength regions: outside the absorbance bands ($\lambda > 290$ nm); in the region about 260 nm which is the main region of absorbance of the nucleic acids; and in the region between 220 and 240 nm. We label the three regions as the scattering region, the nucleic acid region, and the protein region, respectively.

Scattering Region. The pure scattering region is defined as the region of the spectrum in which there are no absorbing chromophores and in which the differential extinction is due to integrated differential scattering. It is the region between 290 and 330 nm. The scattering of circularly polarized light reflects large-order chiral organizations, as has been demonstrated experimentally and theoretically by a series of workers studying the optical activity of large biological structures (Tinoco et al., 1980; Maestre et al., 1982), and it is also a well-known phenomenon in liquid crystals (Holzwarth & Holzwarth, 1977; Bustamente et al., 1984). The reflection bands measured in cholesteric liquid crystals are a reflection of one sense of polarization of circularly polarized light and transmission of light of the opposite sense of polarization.

If this interpretation is correct, then it remains to be explained how the measured CD/CIDS tails are representing structures in each individual cell that must scatter circularly polarized light differentially. These structures could be associated with the state of the cell chromatin since the scattering region CD/CIDS spectrum changes with the cell cycle position. This change seems to reflect changes in the higher order structure of the chromatin. The particles producing the differential scattering could be either the nucleic acids or the protein components of the chromatin, i.e., nucleosomes in various orders of organization. It also could be some other structure associated with the cell division apparatus such as the mitotic spindle or some other alteration of the cytoskeleton. As theory has shown (Bustamante et al., 1982), it is only necessary that the organization is chiral in nature, and this does not necessarily imply that it has to be strictly helical or superhelical. It also could be a microcrystalline structure resembling a twisted ladder.

It is interesting to note in Figure 5 that the G_1-phase and M-phase cell clusters have nearly the same values in the scatter region above 290 nm, implying a similar level of higher order organization. Also in Figure 5, the S–G_2-phase cell cluster has no CIDS contributions above 290 nm, implying little

higher order organization in the cell cycle phase in which chromatin is known to be dispersed.

Nucleic Acid Absorbance Region. The region between 290 and 250 nm has been shown by CD to be one of the most characteristic of the state of nucleic acids in vivo and in vitro (Tinoco et al., 1980). It is in this region that some of the most remarkable changes are seen when the secondary structure of a nucleic acid is altered. Changes from B to A geometry or to Z geometry cause radical changes in the shape and values of the CD curves, and these are very good monitors which can be identified easily for specific cases. In the microscope measurements, the CIDS component is superimposed on the "true" CD signal for a considerable part of the life cycle. However, the CIDS signal is reasonably monotonic in behavior with varying wavelength. This is predicted by theory (Bustamante et al., 1983). The wavelength dependence of the contributions of CIDS to the CD signal are $\approx(1/\lambda^5)\alpha\alpha^*$. The behavior of the polarizability tensor, α, could be described best as

$$\alpha = \sum_{\nu}\alpha_{\nu}(\lambda,\lambda_{\nu,0})$$

where λ is the wavelength of the incident light and $\lambda_{\nu,0}$ is the center of the absorption band of the ν component. At this particular wavelength, $\lambda_{\nu,0}$, there is an "anomalous" change of sign of the scattering contribution. The will indicate the degree of contribution of that particular component of the scatterer (DNA or protein) to the general CIDS scattering pattern, the CIDS contribution to the structure to the general CIDS scattering pattern, and the CIDS contribution to the CD spectra.

Next we study the spectra that have small CIDS scattering contributions. These are associated with the late S and G_2 phases (see the S–G_2 cluster in Figure 5). The feature to note in the S–G_2 spectra in Figure 5 is a positive CD band centered on or about 260 nm. This band is seen usually in the solution CD spectra of dispersed chromatin. It reflects mainly the structure of the nucleic acids and their interaction with the nuclear proteins. In contrast, the M- and G_1-phase DNA region spectra (Figure 3) exhibit large negative values. We interpret this peak suppression as being caused by the large CIDS contributions near 260 nm (see the G_1 and M curves in Figure 5).

Two interpretations follow: (a) The CD at 260 nm is simply measuring the amount of DNA in the cell; and/or (b) a basic change in the structure of the nucleic acids is reflected in the CD changes. The first interpretation is reasonable in the sense that there is an obvious increase in the absorbance measurement in each of the cells as they move from the M phase to the G_2 phase. However, it is possible that the circularly polarized light is differentially transmitted through condensed chromatin structure in the same way that circularly polarized light interacts with liquid crystals. In this sense, it mimics the CD of DNA as it is found in intact bacteriophages after the scattering components have been corrected by devices that increased the acceptance angle of the detectors in regular CD measurements. The suppression of the first CD peak of DNA in such structures has been attributed by some workers as reflecting a possible coiling of the nucleic acids (Gray et al., 1978; Fasman et al., 1978). A different interpretation of these changes in the CD of nucleic acids is given by Hanlon et al. (1984), and this is that it reflects changes in the twisting angles of bases by a small amount toward a more tightly wound DNA.

Protein Region. The largest CD/CIDS changes are measured in the protein region (220–240 nm). At 235 nm, Figure 5 shows dramatic CD/CIDS differences between the G_1 S–G_2 and M phases. The forward CIDS scattering contribution is positive for G_1, nearly zero for S–G_2, and negative for the M-phase cell cluster. These changes cannot represent alterations of the secondary structure of the protein, and the data on the nucleic acids indicate that such large changes are not seen in the regions where only the absorbance bands of nucleic acids are measured. Thus, the most reasonable interpretation is that these changes are alterations in the higher order structure of chromatin and that the main polarizability component that is affecting the differential scattering is that of the protein polarizabilities. It appears that in the chromatin it is the nucleoproteins which do most of the differential scattering and, thus, it is the changes in CIDS and differential scattering components as the cell traverses the cell cycle.

Other structures can also be assumed to cause the changes in the scattering contributions and the large signals measured in the protein region. Among possible candidates are microfilaments and microtubules of the cytoskeleton whose structures might also change in phase with the life cycle of the cell. At present, the CD/CIDS microscopic technique cannot differentiate between the protein structures associated with chromatin and with other proteins.

Models. At present, there is not enough differential scattering information available to try to compute models of specific types of packing of the chromosome in the intact cell. It is obvious that the spatial information as a function of scattering angle cannot be extracted from measurements in the beam mode, i.e., at zero angle of scattering. To obtain that information, differential scattering measurements have to be done on each cell, that is, specific intensities measured at specific angles of the scattered beam. However, certain conclusions can be drawn that might exclude some type of structures, as follows:

(1) There is no apparent directionality of the scattering components; that is, the signals did not depend on the orientation of the cells with respect to the light beam. Thus, the patterns measured for the CHO cells throughout their life cycle are essentially rotationally averaged. This is very important because it says that there is no specific optical axis to the scattering structure. There is no linear dichroism or linear birefringence to complicate the signal, and what is being measured is a differential scattering from a rotationally averaged chiral structure of size and parameters of the order of the light.

(2) The chiral organizations produce scattering tails that are the same order of magnitude as the intrinsic CD of the nucleic acid, and such magnitudes are lower by at least a factor of 10 than the magnitudes obtained from the PSI-type CD spectra observed in some condensed forms of DNA (Tinoco et al., 1980). The condensation of the chromatin in the M phase does not produce the type of crystalline arrangement that presumably exists in the PSI type of particle, and it is probably not as condensed.

An alternative explanation is that the CD/CIDS scattering contributions are due to some other structures, such as components in the cytoskeleton, spindle formation during mitosis, and/or microtubule structures. If so, the alteration, monitored by the CD/CIDS technique, of these structures must be associated in some manner with the cell cycle.

(3) The integrated differential scattering contributions, i.e., the tails to the CD signal, are negative for this type of cell. This is not so for different kind of cells, for example, kangaroo rat kidney tissue culture cells (P. Eremicus), in which the scattering contributions are positive in value throughout most

of the wavelength spectrum (unpublished results).

As the scattering contribution to the signal disappears, the structure either disappears also or changes in organization such that it becomes nonchiral, or the parameters become much larger or much smaller than the range of wavelengths covered by the spectrum.

References

Bustamante, C., Maestre, M. F., & Tinoco, I., Jr. (1980a) *J. Chem. Phys. 73*, 4273.

Bustamante, C., Maestre, M. F., & Tinoco, I., Jr. (1980b) *J. Chem. Phys. 73*, 6046.

Bustamante, C., Tinoco, I., Jr., & Maestre, M. F. (1981) *J. Chem. Phys. 74*, 4839.

Bustamante, C., Tinoco, I., Jr., & Maestre, M. F. (1982) *J. Chem. Phys. 76*, 3440.

Bustamante, C., Tinoco, I., Jr., & Maestre, M. F. (1983) *Proc. Natl. Acad. Sci. U.S.A. 80*, 3568.

Bustamante, C., Keller, D., Maestre, M. F., & Tinoco, I., Jr., (1984) *J. Chem. Phys. 80*, 4817.

Bustamante, C., Maestre, M. F., & Keller, D. (1985) *Biopolymers* (in press).

Cram, L. S., & Holm, D. (1973) *Exp. Cell Res. 80*, 105.

Crissman, H. A., & Tobey, R. A. (1974) *Science (Washington, D.C.) 184*, 1297.

Downing, K. H., & Maestre, M. F. (1979) *Biophys. J. 33*, 68A.

Duysens, L. M. (1956) *Biochim. Biophys. Acta 19*, 1.

Fasman, G. D., & Cowman, M. K. (1978) *The Cell Nucleus Chromatin, Part B* (Bush, H., Ed.) pp 55–57, Academic Press, New York.

Goad, C. A. (1978) *Los Alamos Scientific Laboratory Report LA-7120-MS*, Los Alamos National Laboratory, Los Alamos, NM.

Gray, D. M., Taylor, T. N., & Lang, D. (1978) *Biopolymers 17*, 145.

Hanlon, S., Brudno, S., Wu, T. T., & Wolf, B. (1975) *Biochemistry 14*, 1648.

Holzwarth, G., & Holzwarth, N. A. W. (1973) *J. Opt. Soc. Am. 63*, 324.

Keller, D., Bustamante, C., Maestre, M. F., & Tinoco, I., Jr. (1985) *Biopolymers 24*, 783–797.

Maestre, M. F., & Katz, J. (1982) *Biopolymers 21*, 1899.

Maestre, M. F., Bustamante, C., Hayes, T. L., Subirana, J. A., & Tinoco, I., Jr. (1982) *Nature (London) 298*, 773–774.

Salzman, G. C., Crowell, J. M., Goad, C. A., Hansen, K. M., Hielbert, R. D., LaBauve, P. M., Martin, J. C., Ingram, M., & Mullaney, P. F. (1975) *Clin. Chem. (Winston-Salem, N.C.) 21*, 1297.

Tinoco, I., Jr., Bustamente, C., & Maestre, M. F. (1980) *Annu. Rev. Biophys. Bioeng. 9*, 107–141.

Tinoco, I., Jr., Bustamante, C., & Maestre, M. F. (1982) in *Structural Molecular Biology* (Davies, D. B., Saenger, W., & Danyluk, S., Eds.) p 269, Plenum Press, New York.

Tinoco, I., Jr., Maestre, M. F., & Blustamante, C. (1983) *Trends Biochem. Sci. (Pers. Ed.) 8*, 41.

Tobey, R. A., & Crissman, H. A. (1972) *Exp. Cell Res. 75*, 460.

Tobey, R. A., Anderson, E. C., & Petersen, D. F. (1967) *J. Cell. Physiol. 70*, 63.

Tomlinson, B. L. (1968) Ph.D. Thesis, University of California, Berkeley, CA.

Zeitz, S., Belmont, A., & Nicolini, C. (1983) *Cell Biophys. 5*, 163.

Transbilayer Phosphatidylcholine Distributions in Small Unilamellar Sphingomyelin–Phosphatidylcholine Vesicles: Effect of Altered Polar Head Group†

A. Kumar and C. M. Gupta*

Division of Biophysics, Central Drug Research Institute, Lucknow 226001, India

Received June 4, 1984; Revised Manuscript Received February 14, 1985

ABSTRACT: The effect of the altered polar head group of phosphatidylcholine (PC) on its transbilayer distributions in small unilamellar vesicles containing sphingomyelin (SM) was ascertained with phospholipase A_2 as the external membrane probe. These vesicles were formed by sonication and fractionated by centrifugation. The vesicle size was determined by gel-permeation chromatography and solute entrapment. Experiments were done to confirm that phospholipase A_2 treatments did not induce fusion, lyse the vesicles, or cause PC to migrate across the vesicle bilayer. The complete degradation of external PC in intact vesicles was assured by carrying out the enzyme reactions in the absence as well as in the presence of 9.2×10^{-5} M bovine serum albumin. In small vesicles comprised of SM and 30 mol % 1,2-dipalmitoyl-*sn*-glycero-3-phosphocholine (DPPC), DPPC preferentially distributed in the inner monolayer. This preference of DPPC in these vesicles disappeared upon introducing one C_2H_5 group at the carbon atom adjacent to the quaternary ammonium residue in its polar head group and was reversed when the C_2H_5 group was replaced by C_6H_5 and $C_6H_5CH_2$ substituents or when the P–N distance was increased. These results indicate that the effective polar head-group volume is an important factor in determining the phospholipid distributions across the small vesicle bilayer.

Asymmetric distributions of various membrane components across the membrane bilayer are perhaps essential for differential functioning of the two sides of biological membranes. There is now much evidence to suggest that various membrane constituents are asymmetrically localized in the two leaflets of the membrane bilayer (Op den Kamp, 1979). While this asymmetry is absolute for membrane (glyco) proteins, only partial asymmetry is observed for membrane phospholipids.

† This is Communication No. 3512 from C.D.R.I., Lucknow, India. A.K. was a recipient of a postdoctoral fellowship from the Council of Scientific and Industrial Research, New Delhi, India.

0006-2960/85/0424-5157$01.50/0
